

# Some effects of substrate roughness on wettability

S. J. HITCHCOCK,\* N. T. CARROLL,† M. G. NICHOLAS  
*Materials Development Division, AERE Harwell, Oxfordshire, UK*

The influence of substrate roughness on wettability has been investigated at room and high temperatures using sixteen material combinations, mostly liquid metals and solid ceramics but also water, glycerol and solid nickel. The contact angles assumed by both wetting and non-wetting drops of all but two material combinations increased linearly with the relative steepness of the surface features, the effect being less for experiments conducted at high temperatures. In contrast, the contact angles of good wetting drops of glycerol and exceptionally good wetting drops of Easy-flo decreased when their silica and nickel substrates were roughened. Similarly, contact angles of both wetting and non-wetting drops were decreased by ultrasonic vibration. The experimental data can best be interpreted in terms of the metastable equilibrium configuration models in which an advancing liquid front has to overcome energy barriers associated with surface features. This occurs more readily if these barriers are small relative to the energy of the liquid which our data suggest can be equated with the enthalpy of the liquid. This interpretation enables the effects of substrate roughness at one temperature or with one liquid to be used to predict behaviour at other temperatures and with other liquids.

## 1. Introduction

It has been known for several decades that the wetting of a surface by a liquid is affected by its roughness and this has been exploited in technological developments. Thus early studies with low energy solids and liquids showed that roughening decreased the already small extent to which a non-wetting liquid will spread [1–4]. This phenomenon was used to enhance the water repellency of textiles [1–3]. Recent work with high energy substrates and liquids [5–8] has shown that similar effects occur, and this paper describes a study related to the development of foundry materials and brazing techniques.

The effects of surface roughness on the wetting behaviour of sessile drops, defined by the contact angle subtended at the drop periphery by the liquid surface and the liquid–solid interface as illustrated in Fig. 1, have been carefully considered by several workers, but early theoretical treatments

are in conflict. Wenzel [1] used a thermodynamic approach in which the additional surface area produced by roughening the substrate was regarded as effectively causing an increase in its surface energy and led to the prediction that

$$\cos \theta_R = W_R \cos \theta_0 \quad (1)$$

where  $W_R$  is the roughness area ratio (true area/nominal area),  $\theta_R$  and  $\theta_0$  are the contact angles of sessile drops on rough and smooth horizontal surfaces. This treatment implicitly assumes that the surface features of the substrate are insignificantly small compared to the drop dimensions and that their geometry is of no consequence except in so far as it affects the surface area. In contrast, Shuttleworth and Bailey [9] considered that the asperities on rough surfaces could pose significant barriers to the flow of a liquid attempting to take up the minimum energy contact angle predicted by the Wenzel relationship. By assuming that  $\theta_0$

\*On attachment from Bath University, now with Metal Box Company, Research and Development Division, Wantage, UK.

†On attachment from Bath University, now with Roch Products Ltd, Dunstable, UK.

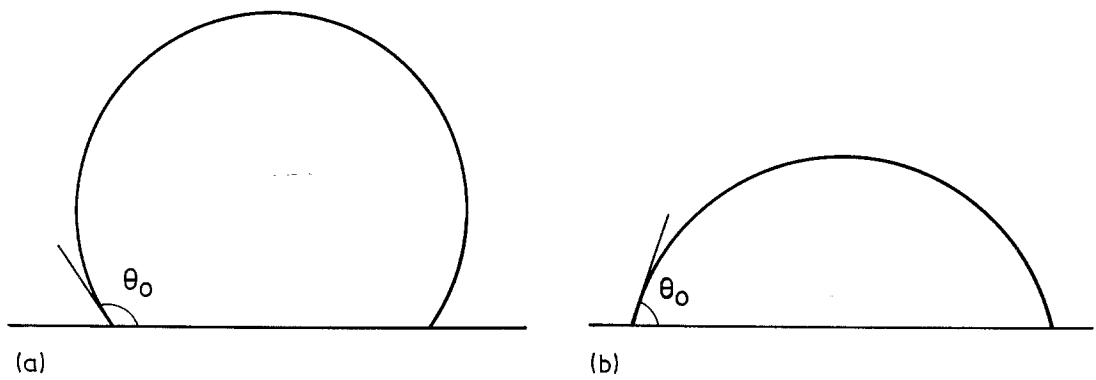


Figure 1 Profiles of (a) non-wetting and (b) wetting sessile drops resting on horizontal substrates. The contact angle,  $\theta_0$ , is subtended by the liquid interface and the liquid–solid interface at the drop periphery.

was an inherent material parameter they concluded that

$$\theta_R = \theta_0 + \alpha_m \quad (2)$$

where  $\alpha_m$  is the maximum slope of the surface feature at the liquid periphery as indicated in Fig. 2. While mathematically,  $\alpha_m$  could be positive or negative and hence  $\theta_R$  greater or less than  $\theta_0$ , considerations of the minimization of the surface energy of the drop led to the conclusion that an advancing liquid front comes to rest on a descending slope and hence that  $\alpha_m$  will be positive, and that a receding front comes to rest on ascending slopes with negative  $\alpha_m$  values.

These treatments lead to conflicting predictions about the effect of surface roughening. The Wenzel model predicts that the contact angles of non-wetting liquids will be increased and those of wetting liquids decreased by roughening a substrate whereas the Shuttleworth and Bailey treatment leads to the expectation that the advancing contact angles of both non-wetting and wetting liquids will be increased. Another significant discrepancy is that the Wenzel model does not predict that surface roughening can cause hysteresis, a difference between the contact angles of advancing and re-

treating liquid fronts, whereas Shuttleworth and Bailey's analysis suggests that this could be twice the maximum slope of the surface features,  $2\alpha_m$ , at the drop periphery.

More recent detailed theoretical analyses, exemplified by those of Dettré and Johnson [10], Huh and Mason [11] and Eick and Good [12], have produced models that incorporate both the Wenzel and the Shuttleworth and Bailey treatments as possible, but not probable, effects of surface roughness. These regard asperities as a series of energy barriers that must be overcome as the liquid front advances from one metastable configuration to another and spreads over the surface. The ability of a liquid to overcome such barriers and spread is regarded as depending on the relative sizes of its vibrational energy and the barriers [13] and as the vibrational energy of the liquid increases, the Wenzel model becomes more applicable than that of Shuttleworth and Bailey.

Because of interest in using surface texturing to modify and control the wetting of foundry materials and brazements, the studies described in this paper were undertaken to provide additional information about the effects of texture on the

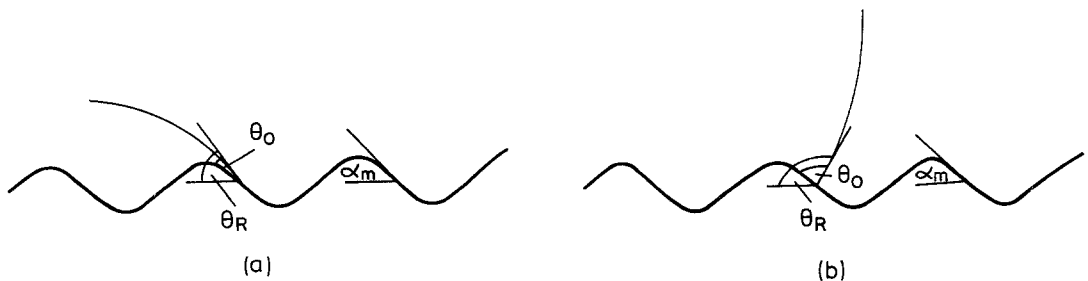


Figure 2 Schematic illustration of the effect of the steepness of surface features on the observed contact angles of (a) wetting and (b) non-wetting drops resting on a rough surface.

TABLE IA Substrates used in this study

Material	Source	Purity	Surface treatment	Topographical characteristics		
				$R_a$ ( $\mu\text{m}$ )	$\lambda_a$ ( $\mu\text{m}$ )	$R_a/\lambda_a$
Alumina	Anderman and Ryder Ltd Electrical Research Association	99.9%	As-sintered	0.78 $\rightarrow$ 2.1	14 $\rightarrow$ 42	0.049 $\rightarrow$ 0.073
		99.99%	As-hot pressed	0.03 $\rightarrow$ 0.046	100	0.0003 $\rightarrow$ 0.0005
Hafnium carbide	Harwell	99.9%	Abraded	0.011 $\rightarrow$ 0.56	12 $\rightarrow$ 100	0.0001 $\rightarrow$ 0.047
Nickel	Rubert and Co. Ltd	99.5%	As-electroformed	0.023 $\rightarrow$ 3.2	45.7 $\rightarrow$ 146.1	0.0005 $\rightarrow$ 0.027
Silica	Harwell	99.9%	Abraded	0.006 $\rightarrow$ 3.1	6.5 $\rightarrow$ 110	0.00006 $\rightarrow$ 0.058
	Rolls-Royce Ltd	--	Sprayed and fired	0.053 $\rightarrow$ 3.3	33 $\rightarrow$ 82	0.016 $\rightarrow$ 0.048
Vitreous carbon	Vitreous Carbon Ltd	99.9%	Abraded	0.001 $\rightarrow$ 0.45	7 $\rightarrow$ 100	0.00001 $\rightarrow$ 0.053

TABLE IB Substrates used in this study

Material	Source	Purity	Surface treatment	Topographical characteristics					
				$W$ ( $\mu\text{m}$ )	$x^*$ ( $\mu\text{m}$ )	$y^*$ ( $\mu\text{m}$ )	$z^*$ ( $\mu\text{m}$ )	$\alpha_m$	$W_R$
Silica	Harwell	99.9%	Photoresist etched cones	60.5 $\rightarrow$ 61.4	40 $\rightarrow$ 54	72.5 $\rightarrow$ 98.5	0.43 $\rightarrow$ 1.21	6.6 $\rightarrow$ 19	1.0010 $\rightarrow$ 1.0036
			Photoresist etched pyramids	112 $\rightarrow$ 116.5	72.5 $\rightarrow$ 98.5	66 $\rightarrow$ 91	0.49 $\rightarrow$ 1.03	8.4 $\rightarrow$ 19	1.0011 $\rightarrow$ 1.0038
			Photoresist etched irregular features	26.7 $\rightarrow$ 53.5	8.4 $\rightarrow$ 11.8	14.5 $\rightarrow$ 31.3	0.2 $\rightarrow$ 5.1	11 $\rightarrow$ 29	1.002 $\rightarrow$ 1.032

\* For explanation of  $x$ ,  $y$  and  $z$  parameters see Fig. 3.

behaviour of high energy substrates and liquids. Most of our experiments were conducted to determine the advancing contact angles assumed at room or higher temperatures by sessile drops of water and several liquid metals resting on model and randomly rough ceramic surfaces. In addition a few experiments were conducted with nickel substrates, and studies of the effects of liquid energy on wetting behaviour were extended by experiments in which sessile drop-substrate systems were ultrasonically vibrated.

## 2. Experimental methods and techniques

The liquids used in the wetting studies were distilled water and glycerol, and spectroscopically pure copper, gallium, mercury, nickel and tin obtained from Johnson Matthey Ltd. The substrates were obtained from a variety of sources as indicated in Tables IA and B. Most of the experiments were conducted with high purity alumina, hafnium carbide, silica or vitreous carbon substrates, but a few employed a porous silica ceramic produced by spraying crushed angular grit mixed with binding agents, and others used electroformed nickel plates. The alumina substrate surfaces were used in the as-received condition, but the textures of the other ceramics were modified. Those of the sprayed silica ceramics were coarsened by firing in air at 1000°C to burn off organic binding agents. A few silica substrates were photoresist-etched using a molybdenum mask to obtain geometrically regular surfaces. Samples of three ceramics, hafnium carbide, silica and vitreous carbon, were abraded on a Lapmaster using 20 μm silicon carbide grit and then partially or completely repolished using 1 μm diamond grit.

In addition to optical and scanning electron microscopy studies, surface textures were characterized using Talysurf\* and Talystep\* surface profilometers. Such traces for photoresist-etched silica samples were used to derive the dimensional parameters identified in Fig. 3 from which values of  $\alpha_m$  and  $W_R$  were calculated. Similarly, the traces for the other rough surfaces were used to derive values for  $R_a$ , the average deviation in height of random points on the surface from a line drawn through the trace such that the cross-sectional areas of asperities above and the grooves below are equal, and  $\lambda_a$ , the average distance



Figure 3 Cross-section of a photoresist etched silica substrate defining parameters whose dimensions are quoted in Tables IA and B.

between the peaks of surface features. The ratio of  $R_a$  to  $\lambda_a$  was used to characterize the geometry of these randomly rough surfaces.

Three types of sessile drop test were conducted to determine the wetting behaviour of the rough substrates. In tests at room temperature, five 0.03 ml drops of water or mercury were deposited from a hypodermic syringe onto levelled substrates and photographed. Before each drop deposition, the substrates were agitated in acetone and dried with a hot air blast. Similarly cleaned substrates and metals were used in high temperature sessile drop tests in which 0.03 ml cylinders of copper, gallium, nickel or tin were placed on substrates located in a vacuum furnace so that they could be seen through observation ports. The furnace chamber was evacuated to  $10^{-3}$ – $10^{-4}$  Pa and power was supplied to a heating element in order to increase the sample temperature by regular intervals while their profiles were being photographed. Except for experiments with gallium, the drops assumed symmetrical profiles with contact angles that did not change measurably after 2 min at temperature, suggesting that equilibrium had been achieved. The data quoted later were obtained from photographs taken 20 min after the experimental temperature equilibrium had been reached. The sessile drops of copper, mercury and water resting on the nickel substrates also had symmetrical profiles, but the marked grain of the substrate caused the contact angle values derived from these profiles to vary with the viewing direction. Finally a few experiments were conducted in air in which Easy-flo\* braze was deposited onto Easy-flo\* fluxed nickel substrates. The braze wetting was good and contact angles had to be estimated from the volume and size of the solidified drops.

Two ultrasonic devices were used in experiments assessing the effects of mechanical energy on wetting behaviour at room temperature, an ultrasonic cleaner with a 50 watt output at a frequency

\*Registered trade names of Rank-Taylor-Hobson Precision Instruments Ltd.

\*Trade name registered by Johnson Matthey Metals Ltd.

of 50kHz and a loudspeaker linked to a signal generator, amplifier and transducer with an output of 2.5 watts at a frequency of 10 to 20 kHz. Drops of mercury or water were deposited onto alumina or silica discs resting on levelled platforms positioned on the vibrating surfaces of the ultrasonic devices. Ultrasonic vibration was applied for 4 min during which time photographs were taken with a 35 mm camera every 15 sec. In a few experiments, a ciné camera was used with a speed of 10 000 frames a second.

The precision of the wetting and surface topography data measured in these various experiments is of significance because of the attempts made later at quantitative comparisons. The contact angles assumed by individual drops in identical conditions did not vary usually by more than plus or minus one or two degrees, and hence the standard error of the means of ten values quoted later was about half a degree or less. An exception to this precision was provided by the data for asymmetric drops of gallium for which the error was two to three degrees. The principal surface topography characteristics measured in this work were  $R_a$  and  $\lambda_a$ , and sampling showed that both parameters could be defined with an accuracy of plus or minus seven or eight per cent. Values for both parameters usually varied from the mean in the same manner, and the standard deviation of the ratio  $R_a/\lambda_a$  was plus or minus ten per cent.

### 3. Experimental results

#### 3.1. Photoresist etched silica substrates

Photoresist etching silica substrates produced model surfaces composed of cubic arrays of regularly shaped, truncated cones or pyramids up to 1.2  $\mu\text{m}$  in height, such as that illustrated in

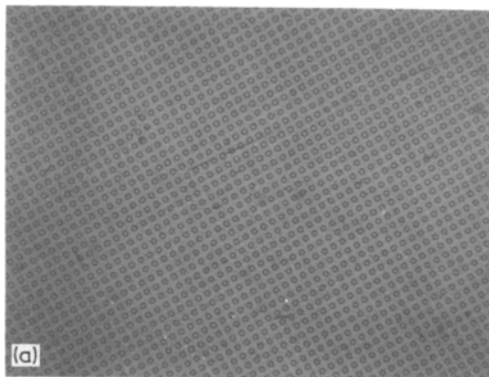


Fig. 4. The surfaces were wetted by water, but not by mercury with sessile drop contact angles ranging from 25 to 43° and 121 to 143° respectively. The largest contact angles were observed for drops of both liquids resting on the substrates with the most steeply sided features and largest Wenzel area ratios.

Detailed comparisons between the wettability and surface topography data are presented in Figs 5 and 6. These show that the cosines of the contact angles of both wetting and non-wetting drops decreased linearly with the Wenzel area ratio, the slopes of the relationships being -5.5 for water and -8.7 for mercury. In contrast, the angles themselves increased linearly with the steepness of the surface features, with data plot slopes of +1.23 for mercury and +0.95 for water.

These experiments at room temperature were supplemented by a few conducted in vacuum at 300 to 500° C using drops of tin resting on heavily etched substrates - with rather irregular surface features up to 5  $\mu\text{m}$  high, as illustrated in Fig. 7. Meaningful  $\alpha_m$  and  $W_R$  values could not be derived but the tin drops were very non-wetting, with contact angles ranging from 154 to 158°. Tin drops resting on the rougher substrates were very mobile and, after solidification, were not attached to the silica. These separated tin surfaces replicated the substrate texture poorly, as shown by comparison of Figs 8 and 7 suggesting that the molten metal had not been in complete contact with the substrate.

#### 3.2. Other ceramics with non-model surface textures

Scanning electron micrographs of ceramics with surface textures produced by sintering, abrasion

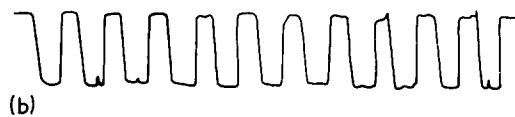


Figure 4 Structure of photoresist etched silica surface with an  $\alpha_m$  of 10.9° and  $W_R$  of 1.0021 revealed by (a) optical microscopy ( $\times 60$ ) and (b) surface profilometry ( $\times 10\ 400$  vertical) and ( $\times 100$  horizontal).

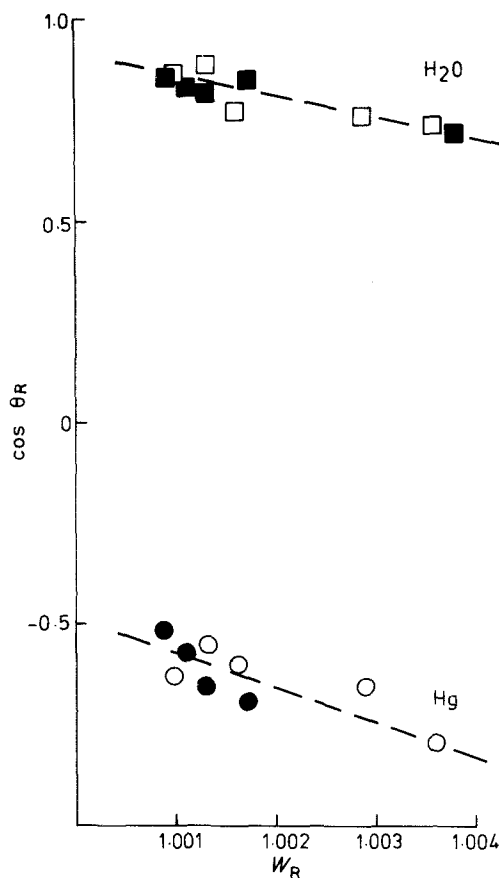


Figure 5 Comparison of the Wenzel area ratios,  $W_R$ , of photoresist etched silica samples with the cosines of the contact angles,  $\theta_R$ , assumed by drops of mercury or water resting on their surfaces. Full symbols refer to surfaces with pyramidal features and hollow symbols to surfaces with conical features.

or spraying are presented in Fig. 9 and the relevant surface profilometry traces are shown in Fig. 10. The structures are chaotic, with random roughness parameters that ranged from 0.001 to  $3.3 \mu\text{m}$  for  $R_a$  and from 6.5 to  $146 \mu\text{m}$  for  $\lambda_a$ . Samples of varying surface roughness were produced for each ceramic, but the micrographs and profilometry traces shown in Figs 9 and 10 relate to surfaces with  $R_a/\lambda_a$  ratios falling within the range 0.036 to 0.056.

\* $(R_a/\lambda_a)$  can be related to  $W_R$  and  $\alpha_a$ , the average inclination of surface features, by expressions of the type

$$W_R = 1 + K_1 (R_a/\lambda_a)^2 \quad (3)$$

$$\alpha_a = \tan^{-1} K_2 (R_a/\lambda_a) \quad (4)$$

where  $K_1$  and  $K_2$  are arithmetic factors equal to about 50 and 9. (For surfaces consisting of close packed arrays of uniform cones, square based pyramids or spherical domes,  $K_1$  is 56.5, 64.6 and 45.4 and  $K_2$  is 11.2, 8.04 and 7.11 respectively.) For  $(R_a/\lambda_a)$  values up to about 0.06, the range of interest in this work,  $\tan \alpha_a$  is a nearly linear function of  $\alpha_a$  and hence Equation 4 can be simplified further to

$$\alpha_a \approx 500(R_a/\lambda_a) \quad (5)$$

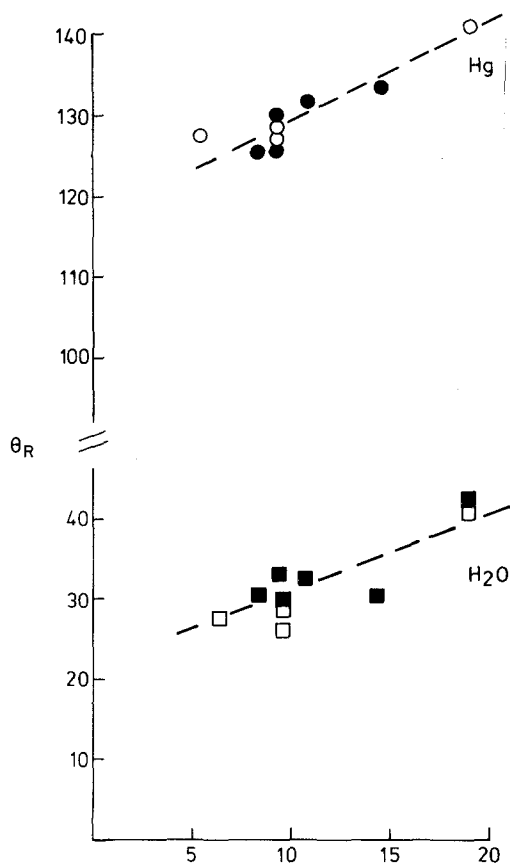


Figure 6 Comparison of the steepness,  $\alpha_m$ , of photoresist etched features on the wetting of silica by drops of mercury or water, as defined by the contact angle  $\theta_R$ . Full symbols refer to surfaces with pyramidal features and hollow symbols to surfaces with conical features.

The irregularity of these ceramics made it impractical to attempt to derive  $\alpha_m$  or  $W_R$  values from the profilometer traces. The surface structures were characterized therefore in terms of the statistical parameters  $R_a$  and  $\lambda_a$ , and their ratio was used as a unique measure of surface texture.\*

More wetting data were obtained for drops of mercury or water resting on abraded silica surfaces at room temperature than for any other systems and Fig. 11 shows that their contact angles

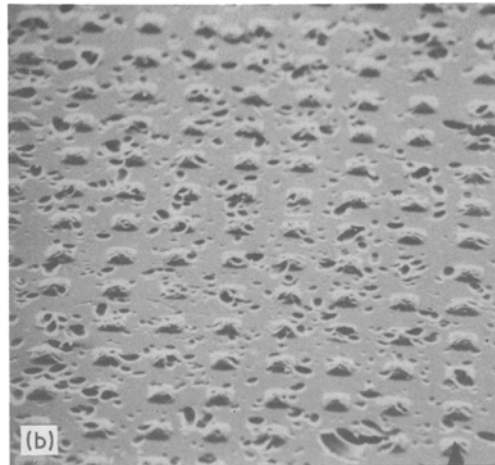
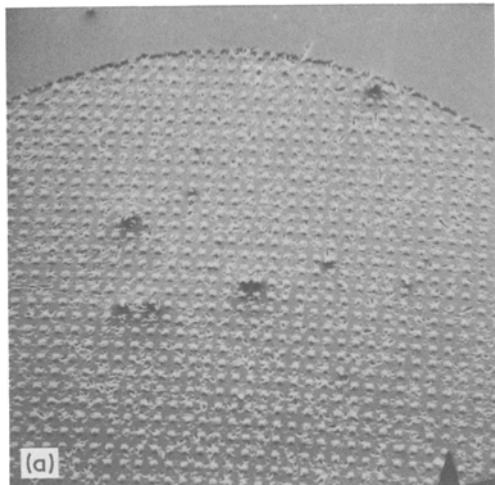


Figure 7 Structure of deeply photoresist etched silica surface as revealed by (a) and (b) scanning electron microscopy ( $\times 42$ ) and ( $\times 164$ ) and (c) surface profilometry ( $\times 3100$  vertical) and ( $\times 124$  horizontal).

exhibited a simple linear dependence on the textural parameter ( $R_a/\lambda_a$ ). For both non-wetting drops of mercury and wetting drops of water, the effect of roughening the silica substrate was to increase their contact angles. The slope of the data plot for mercury was greater than for water, the best fit slopes being  $431$  and  $340^\circ$  respectively, as

summarized in Table II. Also plotted in Fig. 11 are a few data obtained for glycerol which was found to wet the abraded silica well, assuming contact angles that increased with slight surface roughening and then to decrease with ( $R_a/\lambda_a$ ) values in excess of  $0.0108$ .

A second series of experiments showed that the wetting behaviour of drops of mercury or water resting on roughened substrates of other ceramics

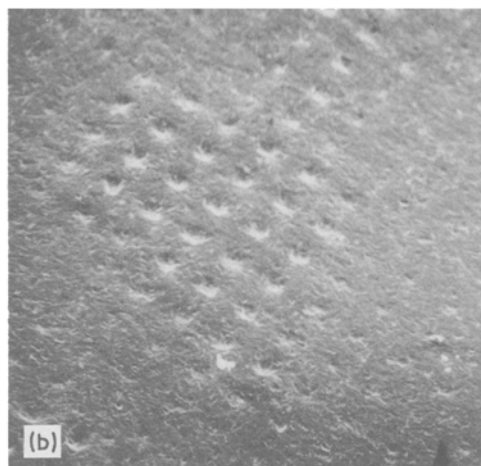
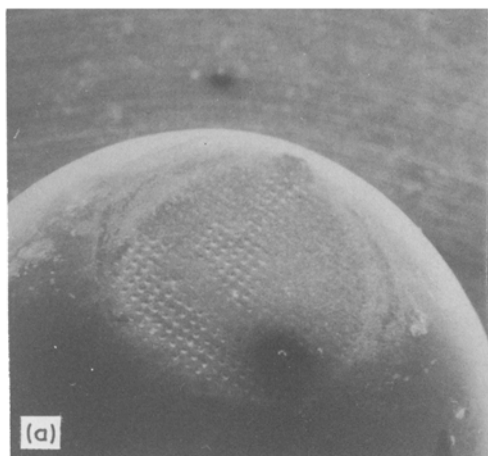


Figure 8 The surface structure of the bottom of a solidified tin drop that had been in contact, at  $500^\circ\text{C}$ , with the silica surface illustrated in Fig. 7, as revealed by (a) and (b) scanning electron microscopy ( $\times 36$ ) and ( $\times 145$ ) and (c) surface profilometry ( $\times 2500$  vertical) and ( $\times 100$  horizontal).

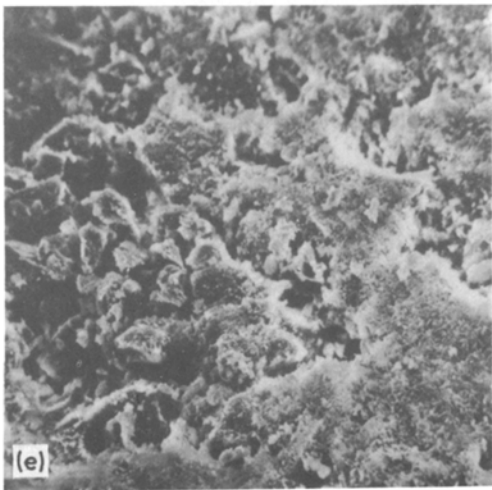
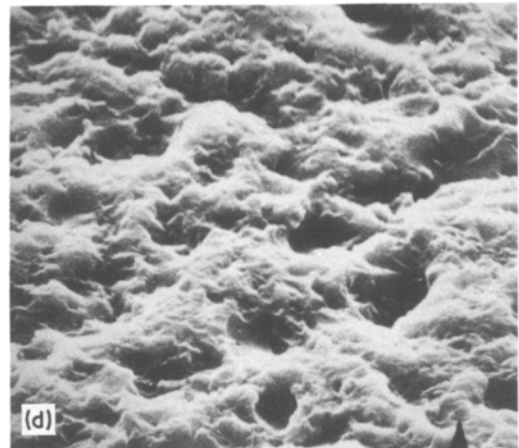
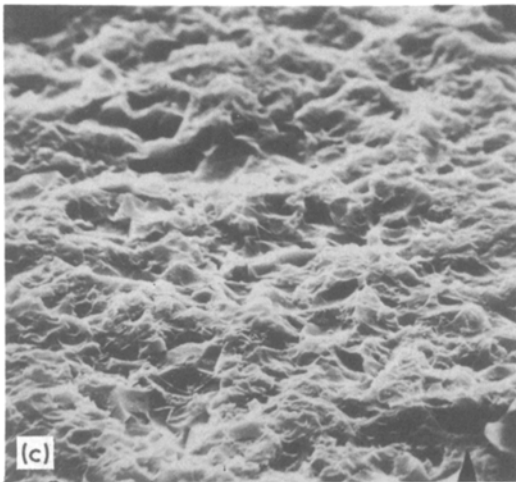
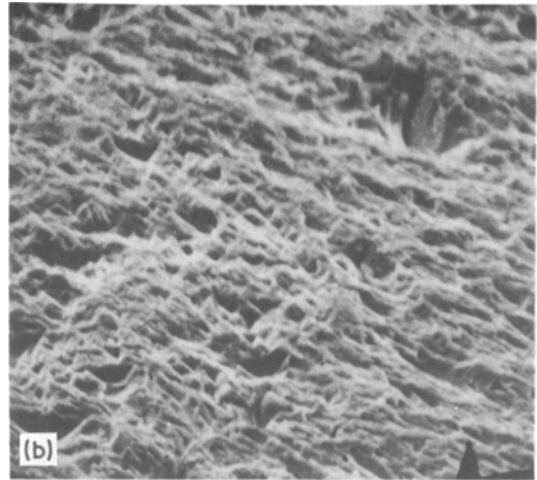
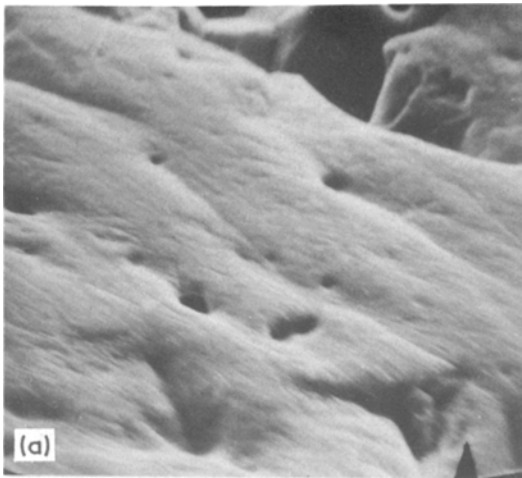


Figure 9 Surface structures of non-model ceramics revealed by scanning electron microscopy (a) alumina ( $\times 1680$ ), (b) hafnium carbide ( $\times 1680$ ), (c) abraded silica ( $\times 1680$ ), (d) vitreous carbon ( $\times 1579$ ) and (e) sprayed angular silica ( $\times 490$ ).

was similar to that observed for silica as shown by the data plotted in Fig. 12. Contact angles of non-wetting drops of mercury and wetting drops of water increased linearly with the parameter  $(R_a/\lambda_a)$ .

The slopes of the relationships were similar to those observed for abraded silica substrates, ranging from about  $350^\circ$  for ceramics wetted by water to about  $450^\circ$  for those contacted by mercury as summarized in Table II.

The third series of experiments with non-model ceramic substrates were conducted in a vacuum furnace at high temperatures using molten drops of copper, gallium, nickel or tin. Some difficulties were encountered during these experiments. Drops of tin and gallium were too mobile to be used with silica substrates having  $(R_a/\lambda_a)$  ratios greater than 0.031. Gallium drops displayed signs of melting at about  $50^\circ\text{C}$  but did not appear.



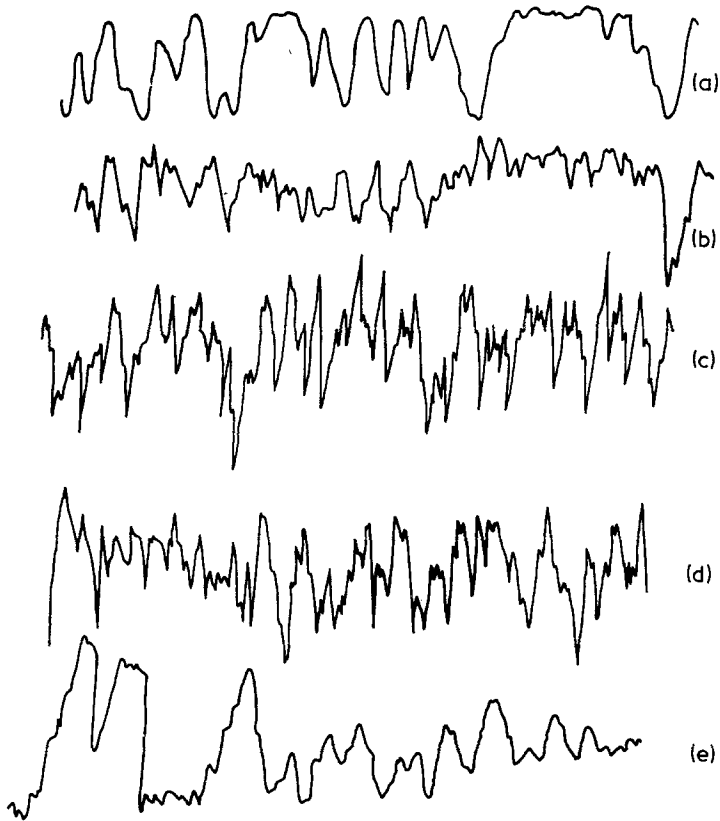


Figure 10 Surface structures of non-model ceramics revealed by (a) alumina ( $\times 2500$  vertical) and ( $\times 100$  horizontal), (b) hafnium carbide ( $\times 50\,000$  vertical) and ( $\times 100$  horizontal), (c) abraded silica ( $\times 10\,000$  vertical) and ( $\times 100$  horizontal), (d) vitreous carbon ( $\times 10\,000$  vertical) and ( $\times 100$  horizontal) and (e) sprayed angular silica ( $\times 250$  vertical) and ( $\times 100$  horizontal).

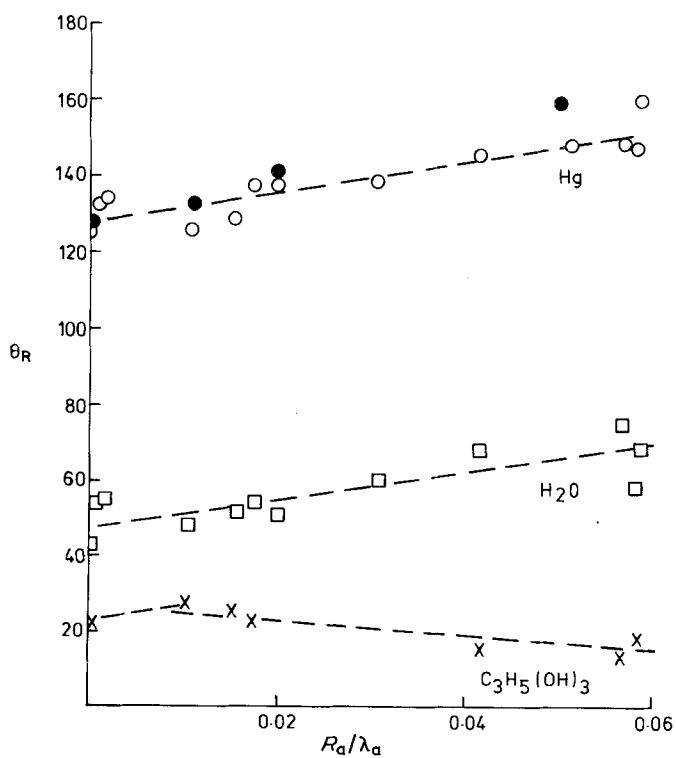


Figure 11 Comparison of the wetting behaviour of drops of mercury, water and glycerol with the roughness of the abraded silica surfaces upon which they rested. The full symbols identify data reported by Tamai and Aratani [5].

TABLE II Parameters describing the wetting behaviour of the roughened substrates used in this study

Liquid	Temperature (°C)	Substrate		C		HfC		Abraded SiO <sub>2</sub>		Sprayed SiO <sub>2</sub>		Ni	
		Al <sub>2</sub> O <sub>3</sub>		$\theta_0$ $d\theta_R/d(R_a/\lambda_a)$		$\theta_0$ $d\theta_R/d(R_a/\lambda_a)$		$\theta_0$ $d\theta_R/d(R_a/\lambda_a)$		$\theta_0$ $d\theta_R/d(R_a/\lambda_a)$		$\theta_0$ $d\theta_R/d(R_a/\lambda_a)$	
		$\theta_0$	$d\theta_R/d(R_a/\lambda_a)$	$\theta_0$	$d\theta_R/d(R_a/\lambda_a)$	$\theta_0$	$d\theta_R/d(R_a/\lambda_a)$	$\theta_0$	$d\theta_R/d(R_a/\lambda_a)$	$\theta_0$	$d\theta_R/d(R_a/\lambda_a)$	$\theta_0$	$d\theta_R/d(R_a/\lambda_a)$
H <sub>2</sub> O	22	-	-	70	293	49	385	47	340	-	-	79	374
Hg	22	118	381	136	465	131	455	128	431	-	-	139	449
Ga	400-800	-	-	-	-	-	-	132	382	-	-	-	-
Sn	400	-	-	-	-	-	-	146	181	-	-	-	-
	600	-	-	-	-	-	-	140	165	-	-	-	-
	800	-	-	-	-	-	-	138	131	-	-	-	-
Cu	1100	-	-	-	-	-	-	-	-	-	-	19	120 (-400)
	1200	-	-	-	-	128	103	-	-	-	-	-	-
Ni	1500	-	-	-	-	-	-	-	-	111	91	-	-
Easy-flo	750	-	-	-	-	-	-	-	-	-	-	6	(-600)

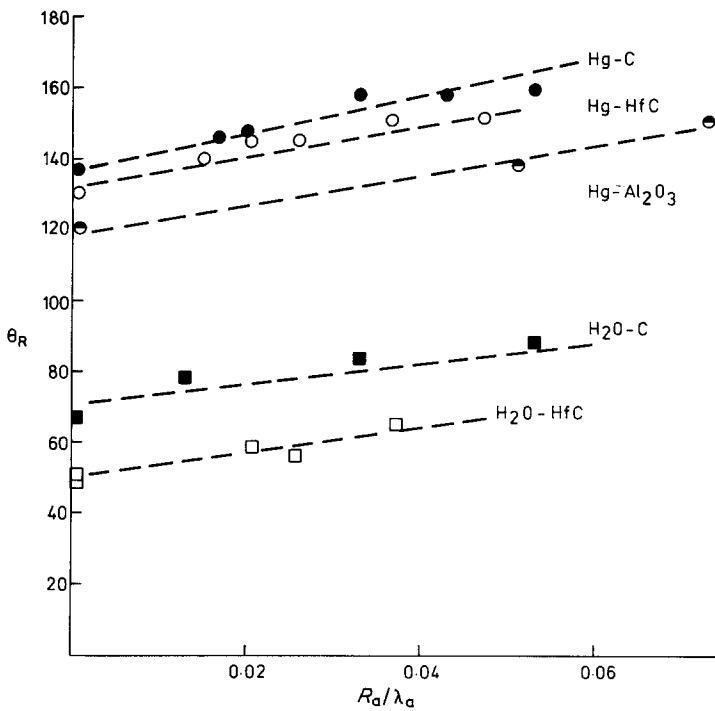


Figure 12 Comparison of the wetting behaviour of drops of mercury and water with the roughness of the ceramic surfaces upon which they rested.

to become fully molten and reflective until about 400°C, and even at 800°C were asymmetrical. However, tin melted at an apparent temperature within a few degrees of its true melting point to form reflective symmetrical drops, nor was any difficulty experienced in forming symmetrical sessile drops of copper or nickel resting on hafnium carbide or sprayed silica substrates.

The rather scattered contact angle values for gallium did not change significantly as the experimental temperature was increased from 400 to 800°C, but those for tin decreased steadily with

temperature in the range 300 to 1000°C as illustrated in Fig. 13. The contact angles for all the molten metals used in this series of experiments were larger on the rougher substrates and Fig. 14 shows that they were a linear function of the ratio  $R_a/\lambda_a$ . The influence of surface roughness on wetting behaviour was different for each metal and, for tin, also varied with the experimental temperature, the greatest effect being displayed by tin at 400°C and the least by nickel at 1500°C, as summarized in Table II.

Many of the metal drops remained attached to

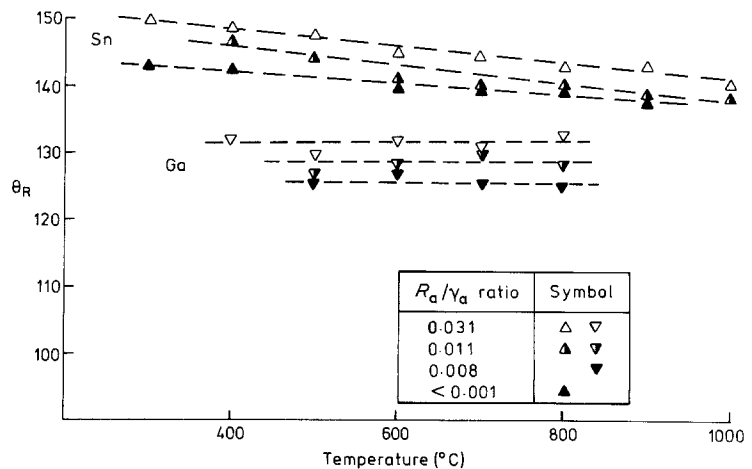


Figure 13 The influence of temperature on the wetting of abraded silica substrates by gallium and tin.

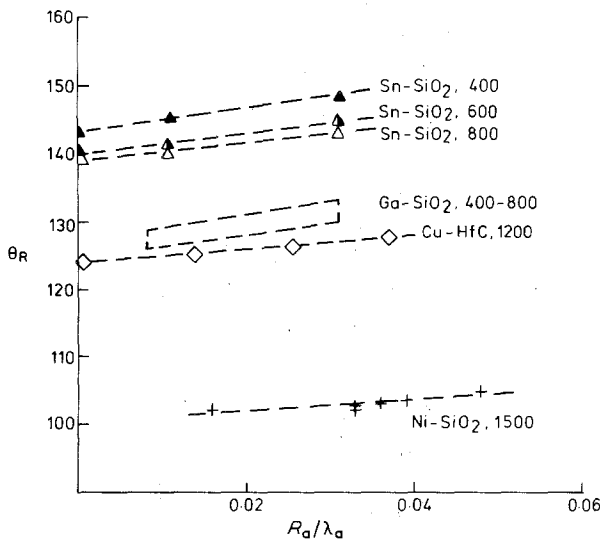


Figure 14 Comparison of high temperature wetting behaviour of drops of molten copper, gallium, nickel or tin with the roughness of the ceramics upon which they rested.

the ceramic substrates after they solidified, but some detached and it was noticed that the bottoms of the drops that had been in contact with very rough substrates were relatively smooth. Thus Fig. 15 shows the bottom surface profile of a tin drop that had been in contact at 500°C with the abraded silica substrate whose texture is illustrated in Fig. 10b.

The final series of experiments with non-model ceramics attempted to assess the influence of ultrasonic vibration on wetting behaviour. Experiments conducted with a 2.5 watt, 10 to 20 kHz source produced no measurable change in the contact angle between mercury and alumina at room temperature even though significant drop distortions were produced by a square wave input as illustrated in Fig. 16. However, using a 50 watt, 50 kHz source caused the contact angles of both mercury and water to decrease linearly with time at 2.6 to 3.2° min<sup>-1</sup> as shown in Fig. 17. Such changes were irreversible, no contact angle increase being observed during a five minute period after power to the vibration source had been switched off.

### 3.3. Electroformed nickel

These substrates had markedly oriented surface textures, as typified by the profilometer traces in Fig. 18, and hence two extreme values of  $R_a/\lambda_a$  were needed to characterize each sample. This substrate directionality was reflected in the wetting behaviour of water and several metals which tended to spread along the grain of the surface, and hence there were also two extreme values of  $\theta_R$ .

The contact angles assumed by non-wetting drops of mercury and wetting drops of water at room temperature advancing across the grain of the substrate surfaces increased linearly with the  $R_a/\lambda_a$  ratios, the slopes of the data plots in Fig. 19 being similar to those reported previously for the wetting of ceramic substrates by these liquids, Table II. The contact angles of the drops of copper advancing across the grain of the nickel substrate surface at 1100°C also increase slowly with the  $R_a/\lambda_a$  ratio, but the contact angles for drops advancing along the grain decreased with the  $R_a/\lambda_a$  ratios. These data are presented in detail in Table III.

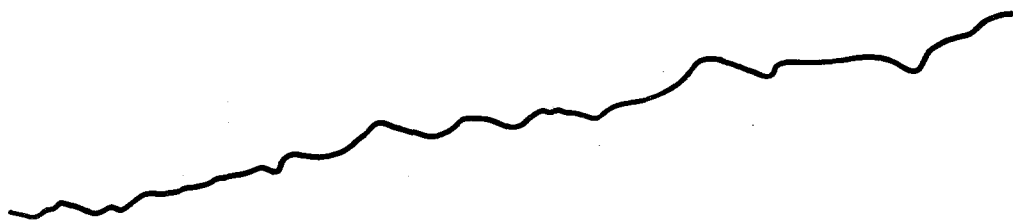
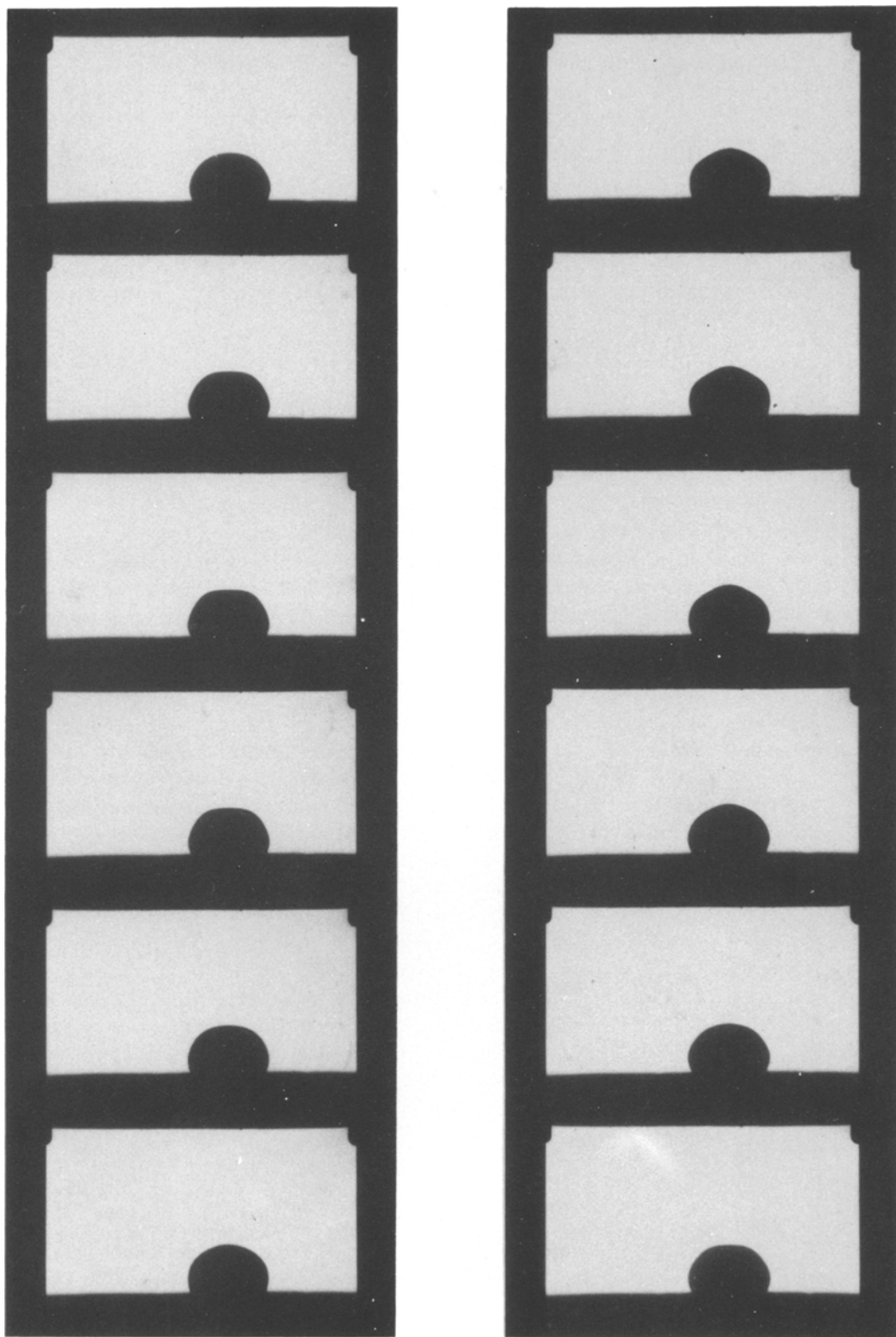
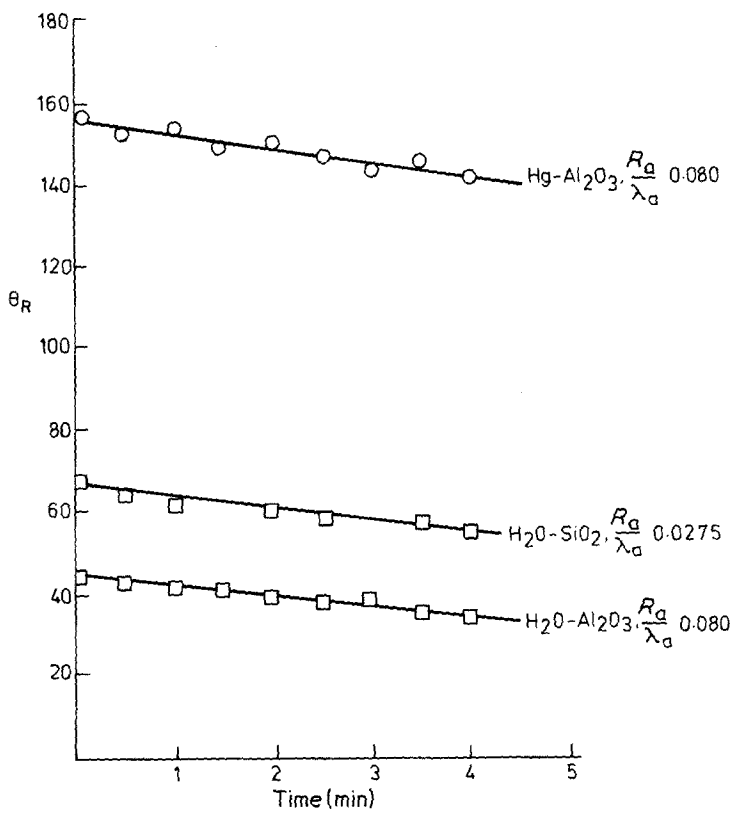


Figure 15 Talystep trace across the bottom of a tin drop that had been in contact with the abraded silica surface illustrated in Figs 9b and 10b (× 500 vertical) and (× 200 horizontal).



*Figure 16* Shapes assumed by a drop of mercury resting on alumina substrate vibrating at a frequency of 10 kHz. Filmed at 10 000 frames a second.

Figure 17 The effect of 50 kHz vibrations on the wetting of rough alumina and silica by mercury or water.



An attempt was made to determine the effect of nickel substrate texture on a very good wetting liquid metal, Easy-flo braze. These experiments had to be conducted under a flux cover and hence contact angle data could not be obtained by direct viewing. However, approximate values were calculated from the dimensions of the solidified drops and it was observed, Fig. 19, that these decreased as the values of the  $R_a/\lambda_a$  ratio derived from both across and along grain surface profilometry became larger.

#### 4. Discussion

This study was designed to provide information about the influence of surface texture on the

wettability of high surface energy substrates, and particularly the wetting of ceramics by molten metals. To this end, the wettability of four ceramics and one metal has been examined with varying thoroughness. Some of the data obtained and presented in the figures comparing wettability and surface texture parameters show significant scatter due to factors mentioned earlier, but the results of the study demonstrate clearly that roughening a substrate usually decreases its wettability. This behaviour was displayed by fourteen of the material combinations examined, the exceptions being the very wetting glycerol-silica and Easy-flo-nickel systems. Such variations from normal behaviour are of particular interest

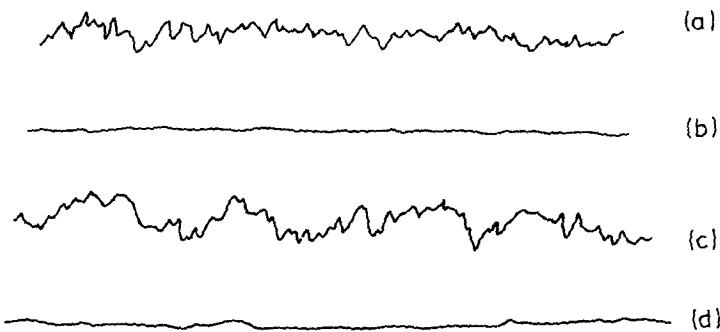


Figure 18 Surface structures of electroformed nickel substrates as revealed by profilometry (a) and (c) across and (b) and (d) along the grain.

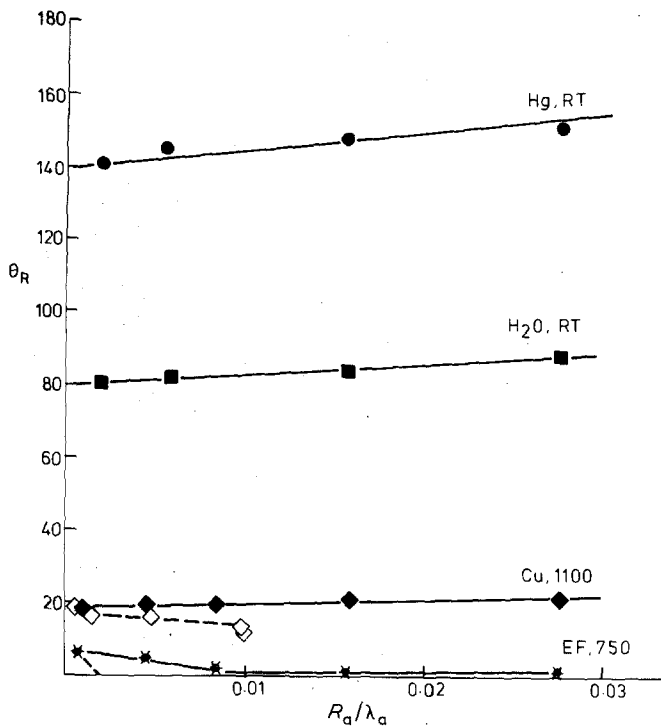


Figure 19 Comparison of the wetting behaviour of several liquids with the roughness of the nickel substrates on which they rested. Dotted lines and hollow symbols refer to along grain spreading, full lines and full symbols to across grain spreading.

because they test the general applicability of theoretical models, and in the case of Easy-flow relate to a technologically important material.

The present work was untypical of most studies of textural effects reported in the literature because it used high surface energy substrates and, often, liquids. However, it is not unique. Thus, a similar quantitative study of the behaviour of the mercury-silica system by Tamai and Aratani [5] and, qualitative studies by Naidich *et al.* [14] and by Crispin and Nicholas [15] for copper and nickel alloys on alumina have been reported. The practice of abrading silica surfaces to produce various roughnesses adopted in this work follows that of

Tamai and Aratani, and it is noteworthy that Fig. 11 shows our data to be in good accord with theirs.\*

Effects of substrate texture on wettability observed in our work are also similar to those found during studies employing low surface energy organic substrates and liquids, work by Oliver *et al.* [6] with mercury deposited on a finely grooved nitrocellulose surface, and Dettré and Johnson [4] with several organic liquids in contact with wax showing that roughening tended to decrease wettability. This conclusion was drawn also by Bartell and Shephard [2, 17] who deposited water and organic liquids onto scribed paraffin surfaces. By using such model textures, Bartell and Shephard and Oliver *et al.* were able to demonstrate experimentally that advancing liquid fronts come to rest on descending slopes, confirming the conclusions reached by Shuttleworth and Bailey [9] in their analysis of the effects of substrate roughening.

There have been many attempts to explain the changes in wetting phenomena produced by substrate roughening. Most attention has been paid to the changes in the contact angles of sessile

TABLE III Surface texture and wetting characteristics of nickel substrates contacted by copper drops at 1100° C

Across grain		Along grain	
$R_a/\lambda_a$	$\theta_R$	$R_a/\lambda_a$	$\theta_R$
0.0009	19	0.001	19.5
0.0044	18	0.0011	17.5
0.0088	18.5	0.0052	16
0.0157	20	0.0056	16.5
0.0275	21.5	0.0098	13.5

\*There is also reasonable agreement between our  $\theta_0$  values and literature data derived from studies not concerned with surface texture effects. Thus Ramqvist [16] reported a  $\theta_0$  value of 132° at 1150° C for the copper-hafnium carbide system as compared to our 128° at 1200° C.

drops and both substrate structure insensitive and structure sensitive models have been developed as exemplified by the early work of Wenzel [1] and of Shuttleworth and Bailey [9]. Our work with photoresist etched silica substrates was specifically intended to generate data that would enable quantitative tests of the models derived from these treatments and examination of Figs 5 and 6 enables comparisons to be made between experimental observations and theoretical predictions. The data plotted in Fig. 5 are in direct conflict with the Wenzel model since they demonstrate that increasing the  $W_R$  value of a substrate decreases its wettability by a wetting liquid, water. Although the  $\cos \theta_R$  values of non-wetting mercury decrease with  $W_R$  is in accord with the Wenzel model, which predicts the slope should be  $\cos \theta_0$ , the experimental slope of  $-8.7$  cannot be interpreted to yield a physically meaningful  $\theta_0$ . In contrast, the linear increase in  $\theta_R$  values of both non-wetting mercury and wetting water drops with  $\alpha_m$  shown in Fig. 6 is in accord with the Shuttleworth and Bailey model. This predicts that the slope of the plots in this figure should be unity, close to the observed slopes of 1.23 for mercury and 0.95 for water. Furthermore, if  $d\theta_R/d(R_a/\lambda_a)$  values for drops of mercury and water resting on abraded silica are divided by 500, (see Equation 5) so that the  $R_a/\lambda_a$  values are converted into approximate  $\alpha_m$  values, near unity gradients of 0.86 and 0.68 are obtained. Similar gradients can be derived by drops of mercury and water resting on other non-model substrates from the data summarized in Table II. Thus the results of our room temperature experiments provide substantial support for the Shuttleworth and Bailey model. However, the effect of substrate roughening on the wetting behaviour of molten metals at high temperatures is less marked, gradients of 0.76 to 0.18 for plots of  $\theta_R$  against  $\alpha_A$  values being suggested by the  $d\theta_R/d(R_a/\lambda_a)$  values summarized in Table II, demonstrating that the Shuttleworth and Bailey model is not entirely adequate.

Other aspects of surface texture induced wetting behaviour observed in this study that have been the subjects of theoretical treatments are the mobility and incomplete liquid–solid contact of drops resting on very rough substrates, the tendency for liquids to spread along the grain of substrates with oriented surface textures, and the changing effect of roughness on the wetting of silica by glycerol. Cassie and Baxter [3] treated the wetting

of very rough, fibrous, substrates and concluded from a consideration of the energetics of various liquid–solid interface configurations that contact could be incomplete and that liquid drops would then be mobile. Their work related to the development of water repellent textiles, and scanning electron microscopy [6] has confirmed the validity of their approach for some model, low energy, surfaces while our work suggests that such effects can be observed also when ceramics contact molten metals. Similarly Shuttleworth and Bailey [9] and Bikerman [18] among others have treated the preferential spreading along the grain, valleys, or an oriented surface texture. Johnson and Dettré [13] argued from a consideration of the energetics of the metastable configurations that might be adopted by a liquid resting on a rough substrate, that spontaneous spreading and wicking will occur if

$$W_R > \frac{1}{\cos \theta_0} \quad (6)$$

which could explain the reversal in the behaviour of glycerol.

This variability in the nature and extent of changes in wetting behaviour produced by substrate roughening has been considered in recent theoretical developments such as those of Johnson and Dettré [13], Huh and Mason [11] and Eick and Good [12] that roughened surfaces present a liquid front with a series of energy barriers between metastable configurations. Thus a liquid will be able to assume the minimum energy configuration predicted by the Wenzel model if its vibrational energy is large compared to that of the barriers, but its wetting behaviour will approach that of the Shuttleworth and Bailey model if this is small. The vibrational energy of a liquid has been discussed but not analysed, by several workers. Johnson and Dettré [13] regarded the vibrational energy of the liquid as an adjustable parameter which could modify the dependence of wetting behaviour on surface roughness defined in terms of the Wenzel area ratio,  $W_R$ , as illustrated in Fig. 20, which can be related to  $R_a/\lambda_a$ . For both wetting and non-wetting liquids, the effect of increasing the vibrational energy is to reduce the rate at which advancing contact angles increase with surface roughening.

The nature of the vibration energy that is relevant to the advance of a liquid front over a rough surface has yet to be identified but our



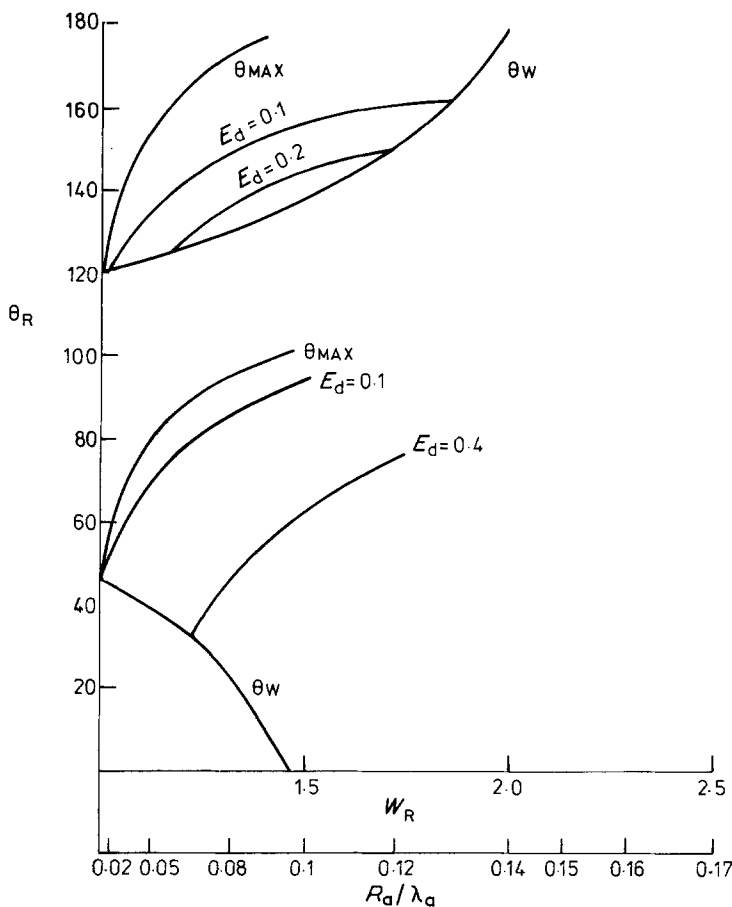


Figure 20 Schematic illustration of the effect of drop energy,  $E_d$ , on the contact angle  $\theta_R$  of wetting and non-wetting drops resting on a model substrate with a surface texture of concentric sinusoidal grooves. After Johnson and Dettre [13].

work suggests that it can be related to the heat content, the enthalpy,  $E_H$ , of the liquid which can be calculated from the expression

$$E_H = \int_0^T C_p dT + L_F \quad (7)$$

where  $C_p$  is the specific heat,  $T$  the temperature and  $L_F$  the latent heat of fusion. This parameter increases with temperature and is different for various liquids at the same temperature, thus possibly accounting both for the decreasing effect of roughening on the wetting behaviour of tin in contact with randomly abraded silica as the experimental temperature was increased from 400 to 1000°C and also for the different effects of substrate roughening on the wetting behaviour of mercury and water at room temperature. Values of  $E_H$  were calculated for different liquids and conditions from reference data [19] and compared with the rate of change in wetting behaviour with substrate roughening. As can be seen from Fig. 21 there is a hyperbolic relationship between the two sets of data, including the rather scattered results

for gallium, that can be described by an expression of the type

$$E_H = \frac{H_s}{(d\theta_R/d[R_a/\lambda_a])} \quad (8)$$

where  $H_s$  is a constant. The curve drawn in Fig. 21 was calculated by assigning a value of 5250 kJ mol<sup>-1</sup> deg<sup>-1</sup> to  $H_s$ , but these peculiar units can be avoided if the ratio  $R_a/\lambda_a$  is converted to an angular slope using Equation 5, in which case  $d\theta_R/d(R_a/\lambda_a)$  becomes a dimensionless parameter and  $H_s$  assumes a value of 10.5 kJ mol<sup>-1</sup>. The consistency of the data plotted in the figure with the empirical equations is such that interpolations and extrapolations can be made with reasonable confidence. That is, the effects of substrate roughening on the wetting behaviour of liquids or at temperatures for which data are lacking can be made with some assurance.

This interpretation of wetting data in terms of energetics can be applied also to the effects of ultrasonic agitation. The lack of effect of 10 or 20 kHz vibrations is in accord with the energetic interpretation of effects produced by substrate

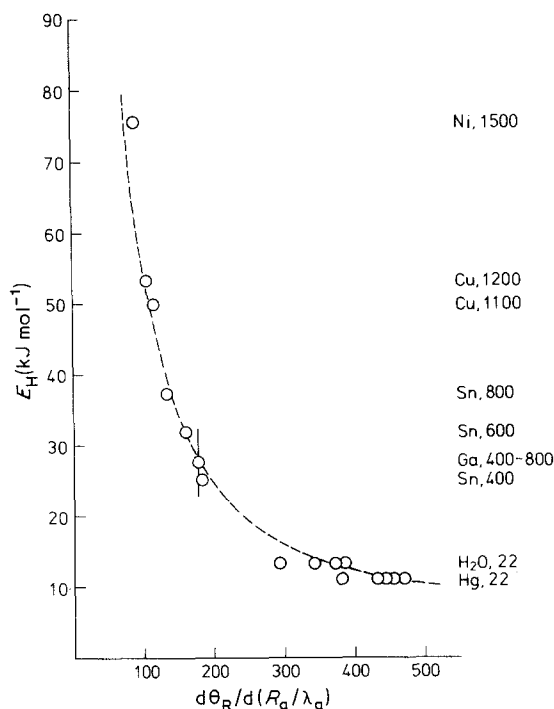


Figure 21 Comparison between the enthalpy of various liquids and the extent to which their wetting behaviour is modified by substrate roughening.

roughness because the total output of the 10 to 20 kHz source was only 2.5 watts which, considering the levelling platform has a mass of 75 g, could have introduced a maximum energy of  $1.6 \text{ kJ mol}^{-1}$  into the mercury and  $0.15 \text{ kJ mol}^{-1}$  into the water drops during the course of the experiments. Both these energies are small compared to the liquid enthalpies and hence could not be expected to have a significant additional effect on wetting behaviour. However the 50 kHz source was twenty times more powerful and hence the total mechanical energy available for conversion into atomic or molecular movements is that much more comparable to the enthalpies of the liquids. Thus it is noteworthy that the contact angle decrease produced by this vibration was more for mercury than for water in accord with its lower enthalpy. Similarly, an energetic interpretation is consistent with the work of Labunov *et al.* [20] showing that the wetting of steel by tin was enhanced by a 22 kHz source with a power of 400 watts and of Smith and Lindberg [21] who found that increasing the output of a 200 to 800 kHz source enhanced the wetting of rough nylon by water.

The contact angle data for roughened substrates obtained during this work from experiments in which the thermal or vibrational energy of sessile drops were varied are, therefore, reasonably consistent with, and explicable by, models that relate the effects to the surmounting of energy barriers. This approach can also account for the mobility of drops on very rough surfaces, for the reversal in the behaviour of glycerol and for the preferential spreading of liquids along the grain of substrates with oriented textures. However, the data obtained in this programme for roughened ceramics refer to at least nominally inert systems, and therefore are untypical of many reactive metal/ceramic combinations involved in technically important processes such as brazing or the containment of molten metal in crucibles. The surface texture of a ceramic may be altered if it reacts chemically with a liquid alloy with which it is in contact, but the few available data relevant to the wetting of ceramics of differing topographies by reactive metal alloys [14, 15] indicate that the initial textures can cause significant differences in wettability.

Our work suggests, therefore, that the production of designed textures can be used in addition to, or instead of, techniques such as changing the temperature or chemistry of the liquid–solid system to modify or control wetting behaviour. However, it is not always convenient or possible to use such approaches in the development of all technologically important processes that depend critically upon wetting characteristics. For example, the opportunity of varying the temperature or chemistry of liquid–solid interfaces encountered in melting and casting processes can be limited severely by economic and safety as well as technical factors. It may be significant, therefore, that the present work demonstrated that it could be possible to decrease the wettability of ceramic crucibles and mounds merely by texturing their surfaces without changing their compositions or the melting and casting conditions.

## 5. Conclusions

(1) Roughening a substrate usually causes its wettability by both wetting and non-wetting liquids to decrease. Exceptions to this generalization occur if the liquid is inherently very well wetting or the surface texture very rough.

(2) The contact angles of both wetting and non-wetting liquids often increase linearly with the

substrate surface texture parameter  $R_a/\lambda_a$  where  $R_a$  is the average amplitude and  $\lambda_a$  the average wavelength of the surface features.

(3) The effect of surface roughening on wetting behaviour is lessened if the thermal or mechanical energy of liquid drops is increased by raising their temperature or subjecting them to ultrasonic vibration.

(4) An empirical relationship exists between the enthalpy of a liquid and the extent to which its wetting behaviour is changed by substrate roughening which allows predictions to be made about the behaviour of uninvestigated liquids.

(5) The development of certain types of surface roughness may be usefully applied in the improvement of foundry materials.

### Acknowledgements

The authors are grateful for the financial support given to the Metals and Chemical Technology Centre by the Engineering Materials Requirements Board of the Department of Industry. They have also benefited from useful discussions held with Mr D. Ford of Rolls-Royce Ltd and with Drs D. T. Livey and G. McHugh of the Coatings and Interface Technology Group at Harwell. The early work of B. J. Dunbar who helped to establish some of the techniques employed is much appreciated.

### References

1. R. N. WENZEL, *Ind. Eng. Chem.* **28** (1936) 988.
2. F. E. BARTELL and J. W. SHEPHARD, *J. Phys.*

- Chem.* **57** (1953) 211.
3. A. B. D. CASSIE and S. BAXTER, *Trans. Farad. Soc.* **40** (1944) 546.
4. R. H. DETTRÉ and R. E. JOHNSON, *Adv. Chem. Ser. No. 43* (1963) 136.
5. Y. TAMAI and K. ARATANI, *J. Phys. Chem.* **76** (1972) 3267.
6. J. F. OLIVER, C. HUH and S. G. MASON, *J. Adhesion* **8** (1977) 223.
7. *Idem*, *Colloids and Surfaces* **1** (1980) 79.
8. J. F. OLIVER and S. G. MASON, *J. Mater. Sci.* **15** (1980) 431.
9. R. SHUTTLEWORTH and G. L. J. BAILEY, *Disc. Farad. Soc.* **3** (1948) 16.
10. R. H. DETTRÉ and R. E. JOHNSON, *Adv. Chem. Ser. No. 43* (1963) 112.
11. C. HUH and S. G. MASON, *J. Colloid Interface Sci.* **60** (1977) 11.
12. J. D. EICK and R. J. GOOD, *ibid.* **53** (1975) 235.
13. R. E. JOHNSON and R. H. DETTRÉ, *Surf. Colloid Sci.* **2** (1969) 82.
14. YU. V. NAIDICH, V. Z. ZHURALEV, G. G. CHUPRINA and L. V. STRASHINSKAYA, *Sov. Pow. Met. Met. Ceram.* **12** (1973) 895.
15. R. M. CRISPIN and M. G. NICHOLAS, *J. Mater. Sci.* **11** (1976) 17.
16. L. RAMQVIST, *Int. J. Powder Met.* **1** (1965) 2.
17. F. E. BARTELL and J. W. SHEPHARD, *J. Phys. Chem.* **57** (1953) 455.
18. J. J. BIKERMAN, *J. Colloid Sci.* **5** (1950) 349.
19. JANAF Thermochemical Tables, NBRDS, National Bureau of Standards, Washington DC, Vol. 37 (1970).
20. V. A. LABUNOV, N. I. NAILOVICH and I. N. LASHCHENKO, *Zavodskaya Lab.* **42** (1976) 817.
21. T. SMITH and G. LINDBERG, *J. Colloid Interface Sci.* **66** (1978) 363.

Received 26 June and accepted 4 August 1980.